SINERGI Vol. 30, No. 2, June 2026: 397-410
http://publikasi.mercubuana.ac.id/index.php/sinergi
http://doi.org/10.22441/sinergi.2026.2.007

Extrusion parameter optimization to improve the mechanical performance of recycled PLA-PETG blends using Taguchi-GRA approach

Annisa Fatimatus Zahro[1], Ihwan Ghazali[2] , Achmad Pratama Rifai[1], Wangi Pandan Sari[1]*
[1]Department of Mechanical and Industrial Engineering, Faculty of Engineering Universitas Gadjah Mada, Indonesia
[2]Faculty of Industrial and Manufacturing Technology and Engineering, Universiti Teknikal Malaysia Melaka, Malaysia

Abstract
Recycled polymers offer a promising pathway toward sustainable additive manufacturing, but their mechanical performance is often limited by degradation and incompatibility between mixed materials. This study investigates the optimization of extrusion parameters for recycled PLA–PETG blends to improve tensile strength and ductility. The Taguchi method was applied to efficiently evaluate the effects of PLA content, temperature, and extrusion speed, while Grey Relational Analysis (GRA) was incorporated to enable simultaneous optimization of tensile strength and elongation, which cannot be achieved using Taguchi alone. The Taguchi–GRA approach identified 30 wt% PLA, 225 °C, and 300 mm/min as the optimal parameter set, producing filament with a tensile strength of 7.47 MPa and elongation of 1.58%, corresponding to a ~28% improvement over the lowest-performing condition. Although the optimized recycled filament exhibited significantly lower properties than commercial PETG, the performance is adequate for low-stress functional applications such as prototyping components and non-load-bearing parts. Fractographic analysis further revealed poor interlayer and interfacial adhesion, explaining the limited ductility of the recycled blends. These findings demonstrate that combining Taguchi and GRA provides a practical route for balancing strength and ductility in sustainable filament development and provides a foundation for future improvements through the use of compatibilizers, post-processing, and enhanced extrusion control.

Keywords:
3D printing;
Extrusion optimization;
Fused Deposition Modelling;
Mechanical properties;
Recycled PETG;
Recycled PLA;
Sustainable manufacturing;
Taguchi-GRA;

Article History:
Received: May 21, 2025
Revised: November 24, 2025
Accepted: December 17, 2025
Published: June 3, 2026

Corresponding Author:
Department of Mechanical and Industrial Engineering, Faculty of Engineering Universitas Gadjah Mada, Indonesia
Email:
wangipandansari@ugm.ac.id

INTRODUCTION

Additive manufacturing (AM), more commonly known as 3D Printing (3DP), has experienced rapid growth since its development in the late 1980s. This technology plays a crucial role in research environments by significantly simplifying the prototyping process. It has also been widely used in various sectors such as automotive [1][2] , aerospace [3][4] healthcare [5][6], and consumer products [7][8]. For example, aerospace and automotive companies leverage AM to produce lightweight components with intricate designs that are difficult to achieve via conventional methods. At the same time, the healthcare sector uses AM for patient-specific implants and anatomical models [9][10]. The consumer market has also embraced 3D printing for personalized goods and prototyping, including fashion [11].

The global AM industry was valued at roughly $26.79 billion in 2024 and projected to continue on a strong upward trajectory, reaching over $189.34 billion by 2034 with an estimated ~21.6% compound annual growth rate [12]. Such

optimistic forecasts underscore the transformative impact of 3D printing, as manufacturers increasingly integrate AM into their production workflows in automotive and aerospace supply chains, medical device fabrication, and even end-user consumer applications. The advancement and adoption of additive manufacturing technologies solidify their in the future in manufacturing. However, along with its benefits, the widespread use of 3D printing raises sustainability concerns, particularly regarding waste generation. Additive manufacturing is often lauded for being more material-efficient than subtractive method, as it does not involve cutting away excess material [13][14] and it can reduce material waste by up to 55% compared to traditional forging methods [15]. Yet, AM is not a zero-waste process.

The 3D printing workflow inherently produces various plastic wastes, including support structures, rafts, failed prints, and purged filament. These are usually necessary to ensure print stability and quality (for instance, supports for overhanging features), but after printing they are removed and discarded. Studies have noted that support materials and failed prints constitute a substantial portion of 3D printing waste, which contributes significantly to environmental pollution if not managed properly [16]. For example, a campus makerspace recycling program observed that everyday operation of FDM printers generates large boxes of PLA support scraps and rejected prints in a short time [17]. This waste stream poses an environmental challenge, especially as AM usage scales up. Reducing and recycling 3D printing waste has therefore become a priority for sustainable manufacturing initiatives. Indeed, there is a growing interest in developing circular economy approaches for AM, capturing used or discarded filament material and reprocessing it into new filament, as a strategy to mitigate plastic waste and reduce the need for virgin materials in 3D printing [18].

Material choice plays a pivotal role in both the performance of printed parts and their end-of-life recyclability. Among the most widely used materials in additive manufacturing, particularly in Fused Deposition Modeling (FDM) or Fused Filament Fabrication (FFF)—the most commonly adopted AM technologies due to their ease of use and relatively low cost [19][20], are the thermoplastics polylactic acid (PLA) and polyethylene terephthalate glycol-modified (PETG) [21]. PLA is a biodegradable polyester derived from renewable resources (such as corn starch), known for its ease of printing and decent rigidity [22]. It has become the “go-to” filament for beginners and is heavily used for prototypes, educational models, and consumer products due to its low warping and good detail reproduction [22][23]. Typical applications of PLA extend beyond printing into traditional manufacturing – for instance, as an implant material and for bone repair [22][24]. PETG, on the other hand, is a glycol-modified version of PET (commonly used in water bottles) and is more widely favored for 3D printing due to its enhanced processing characteristics [25]. It offers ease of processing and also exhibits high chemical resistance, dependable tensile toughness, and good flexibility [26]. PETG’s mechanical resilience and chemical stability make it popular for printing functional parts that require durability, such as mechanical components, brackets, and containers that may undergo stress or contact with liquids [27][28]. Both PLA and PETG are thermoplastics, which means they can be melted and remolded, theoretically allowing them to be recycled into new filament feedstock. In practice, PLA’s biodegradability means it can be industrially composted at end-of-life or reclaimed and re-extruded – though it needs specific conditions to degrade efficiently [29, 30, 31]. PETG is a petroleum-derived plastic but is 100% recyclable as well – when reprocessed or fully combusted it leaves no toxic residue (only carbon dioxide and water) [32]. These attributes make PLA and PETG attractive from a sustainability perspective, provided that effective recycling systems are in place.

Despite their recyclability, challenges arise when attempting to recycle and reuse PLA and PETG filaments, especially related to degradation of material properties. One major issue with PETG is its hygroscopic nature, it readily absorbs moisture from the environment [33]. During printing, any absorbed moisture in the filament can cause hydrolysis (polymer chain breakdown), leading to defects such as bubbles, weak layer bonding, and diminished mechanical strength in the printed part [34][35]. PETG’s sensitivity to humidity means that recycled PETG must be carefully processed to avoid additional thermal and hydrolytic degradation each time it is re-melted. Studies have observed that PETG can suffer notable drops in properties like tensile strength after even one recycling cycle due to the moisture-induced degradation process [34, 36, 37]. PLA is less moisture-sensitive by comparison (it is more dimensionally stable and prints reliably without drying in most conditions), but PLA has its drawback of being relatively brittle. In the context of recycled filament, pure PLA recyclate can become more brittle after multiple reprocessing cycles as the polymer

chains shorten [18]. Thus, each material alone has limitations when recycled: PETG tends to lose strength due to moisture-related degradation, and PLA can become too brittle, limiting its reuse in load-bearing applications. Additionally, PLA and PETG are inherently immiscible polymers, resulting in weak interfacial adhesion and phase separation when blended [38][39], which further reduces ductility and tensile performance.

To address these issues, recent research and development efforts have explored blending PLA and PETG – combining both polymers, to create improved recycled filaments [36, 40, 41]. The rationale for PLA–PETG blends is to capitalize on the complementary properties of the two materials. PLA provides rigidity and higher tensile strength, whereas PETG contributes ductility and toughness. By mixing them, the aim is to achieve a recycled filament that retains sufficient stiffness from PLA while also gaining impact resistance and flexibility from PETG. This could mitigate PLA's brittleness with PETG's toughness and simultaneously counteract PETG's moisture weakness by diluting it with PLA (which could reduce the overall water uptake of the blend). In essence, a properly engineered PLA/PETG recycled blend could exhibit balanced mechanical properties superior to either material alone in recycled form. Preliminary studies support this approach: for instance, recycled PETG has been shown to have excellent impact durability but lower strength compared to PLA, suggesting a blend can bridge the gap [18]. Likewise, blends of other recycled polymers have shown improved tensile properties when a second polymer is introduced to enhance intermolecular strength [42]. Therefore, developing a PLA–PETG hybrid filament from waste streams aligns with the goals of sustainable manufacturing: it seeks to extend the life of 3D printing plastics and reduce waste, without compromising the functional performance needed for practical applications. However, achieving such balance can be dependent on extrusion parameters, such as temperature, shear rate, and mixing conditions, which may affect the final blend morphology and performance [43][44].

While PLA and PETG recycling have been independently studied [16, 36, 45, 46], few investigations have optimized processing conditions specifically for PLA–PETG blends derived from recycled materials Moreover, few studies systematically apply multi-response statistical frameworks, such as the Taguchi method integrated with Grey Relational Analysis (GRA), to address the trade-off between tensile strength and ductility. GRA enhances the Taguchi method by allowing multiple outputs to be evaluated simultaneously via a single response index [47][48], which can help identify a parameter set that offers balanced mechanical performance. Therefore, this study applies a Taguchi–GRA framework to identify optimal extrusion conditions that enhance both tensile strength and ductility of recycled PLA–PETG blends, addressing the immiscibility and degradation challenges while filling the methodological gap in multi-response optimization for sustainable filament development.

METHOD

Material

The raw materials used in this study were post-consumer PETG and PLA waste, collected from a local 3D printing vendor. The waste materials consisted of failed prints, support structures, and end-of-life parts commonly produced in desktop FDM applications. These were manually sorted and cleaned to remove dust, oils, and contaminants that might affect material quality. The PETG and PLA waste materials were then cut into smaller fragments no larger than 3 mm using a mechanical cutter. This particle size was selected to ensure compatibility with the filament extruder feed system, and the shredded materials were categorized as recycled PETG (rPETG) and recycled PLA (rPLA) pellets.

Prior to extrusion, moisture removal was conducted through oven drying, which is critical to prevent the formation of air bubbles, poor interlayer bonding, and other defects during the melt-extrusion process. The rPLA pellets were dried at 120 °C for 1.5 hours, while the rPETG pellets were dried at 100 °C for 30 minutes. After drying, both materials were immediately sealed in airtight containers and stored in a dry environment to prevent moisture reabsorption. Blending was carried out by manually weighing and mixing the two types of pellets in designated ratios. This study investigated three main process parameters: PLA content (%), extrusion temperature (°C), and extrusion speed (mm/min). Each parameter was tested at three levels, as shown in Table 1.

Table 1. Influencing factors and level for each factor

Factor	Level		
	1	2	3
PLA content (%)	0	30	50
Extrusion temperature (°C)	220	225	230
Extrusion speed (mm/min)	300	387.5	475

The filament extrusion was performed using a Wellzoom single-screw filament extruder, which is designed for small-scale research and prototyping. This extruder includes a digital temperature control system, variable speed motor, and a standard 1.75 mm nozzle die. As the rPETG–rPLA blend was fed into the hopper, it passed through a heated barrel and was extruded through the nozzle. The molten filament was cooled naturally in ambient air under consistent room-temperature conditions to minimize thermal variation during solidification. The extruded strands were collected manually and filament diameter uniformity was monitored using calipers at multiple points along each strand. The targeted filament diameter was 1.75 ± 0.2 mm, which is compatible with most consumer-grade FDM 3D printers. The overall research procedure is summarized in the flowchart shown in Figure 1.

Experimental Design and Characterization

The experimental design followed the Taguchi method, which is an efficient statistical tool to determine optimal process parameters with minimal experimentation. Instead of conducting complete factorial experiments, an L9 orthogonal array (OA) was employed, which allows the study of three parameters at three levels each using only nine experimental runs. The matrix of parameter combinations is shown in Table 2.

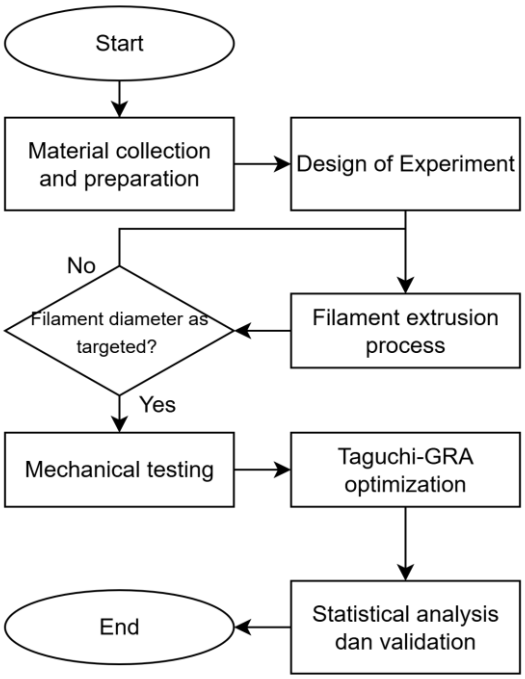

Figure 1. Research flowchart

To account for variation, each run was repeated three times, resulting in a total of 27 specimens.

Tensile testing of the extruded filament was conducted using a CRN-50 Universal Testing Machine (Carson Technology Testing Equipment Co. Ltd.). Straight filament strands were cut to a length of 150 mm and tested at a tensile speed of 0.5 mm/min to determine mechanical properties including Ultimate Tensile Strength (UTS) and Elongation at break. Testing was performed under consistent laboratory conditions to minimize environmental variability.

For validation purposes, a confirmatory test was performed using the optimal combination of PLA content, extrusion temperature, and extrusion speed identified via optimization. The corresponding filament was then used to print standardized tensile specimens using an FDM 3D printer following ASTM D638 Type IV geometry. The dimensions of the printed specimens were 115 mm × 19 mm × 3.2 mm, as shown in Figure 2. The printing was carried out using a nozzle temperature of 235 °C and a bed temperature of 70 °C, with a layer height of 0.25 mm, printing speed of 70 mm/s, infill density of 100%, and wall thickness of 0.8 mm. The tensile test was conducted at a crosshead speed of 2 mm/min. Additionally, fracture surface morphology of the printed specimens was analyzed using a Dino-Lite/1.3 MP AF4915 digital microscope, and image processing was conducted using ImageJ software.

Table 2. L9 orthogonal array

Run	PLA content (wt%)	Extrusion Temp (℃)	Extrusion Speed (mm/min)
1	0	220	300
2	0	225	387.5
3	0	230	475
4	30	220	387.5
5	30	225	475
6	30	230	300
7	50	220	475
8	50	225	300
9	50	230	387.5

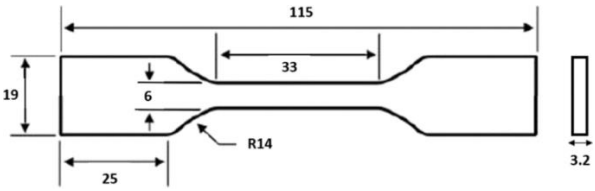

Figure 2. Specimen dimension according to ASTM D638 type IV standard

The combined Taguchi–GRA framework was adopted because UTS and elongation at break represent competing performance objectives, necessitating a multi-response optimization method to determine an optimal balance. The experimental structure used in this study is summarized in Figure 3, which outlines the role of input parameters, controlled and uncontrolled factors, and target output responses within the Taguchi–GRA framework.

Statistical Analysis and Optimization

To analyze the influence of each parameter on tensile performance, experimental results were transformed into signal-to-noise (S/N) ratios. In Taguchi methodology, S/N ratios help quantify the effect of each factor on the response variable by maximizing the desired signal while minimizing variability (noise). Since the objective of this study was to maximize tensile properties, the “larger-is-better” S/N ratio was used. The S/N ratio (η) was calculated using (1), where η equals to S/N ratio, n represents the number of repetitions, and Y_i represents the i^{th} individual experiment result.

$$\eta = -10 \log\left[\frac{1}{n}\sum_{i=1}^{n}\frac{1}{Y_i^2}\right] \quad (1)$$

To determine the statistical significance of each main factor and interaction, Analysis of Variance (ANOVA) was conducted. Before performing ANOVA, the normality of residuals was evaluated to confirm the suitability of parametric analysis. The significance threshold was set at $p < 0.05$. The hypotheses used in ANOVA were:

H_0: The factor has no significant effect on the response.

H_1: The factor has a significant effect on the response.

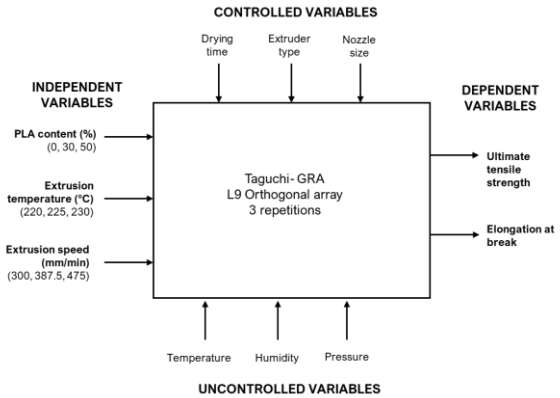

Figure 3. Research model illustrating the experimental structure using Taguchi–GRA with L9 orthogonal array

ANOVA results provided the percentage contribution of each factor, allowing prioritization of the most influential parameters on filament performance.

To account for multiple performance criteria, Grey Relational Analysis (GRA) was employed for multi-response optimization. GRA allows multiple outputs to be transformed into a single comprehensive metric, the Grey Relational Grade (GRG), enabling identification of parameter settings that yield the best overall performance.

The first step in the GRA procedure involved data normalization, which was necessary to make all responses dimensionless and comparable regardless of their original scale. Since all responses were to be maximized, the "larger-the-better" normalization method was applied, as shown in (2). Here, x_{ij}^* is the normalised value, $x_{ij}$is the original S/N ratio value and $\min(x_{ij})$ and $\max(x_{ij})$ are the minimum and maximum values of the j-th performance characteristic.

$$x_{ij}^* = \frac{x_{ij} - \min(x_j)}{\max(x_{ij}) - \min(x_{ij})} \quad (2)$$

Next, the Grey Relational Coefficient (GRC) was calculated to determine how closely each experiment’s normalized value approached the ideal target. The deviation from the ideal and the GRC are computed using Equations (3) and (4), respectively, where x_0^* the reference (ideal) value, usually 1 for “larger-the-better”; Δ_{ij} is the absolute difference between the ideal and the normalized value; Δ_{min} and Δ_{min} are the minimum and maximum deviations across all runs and responses; and ζ is the distinguishing coefficient, set to 0.5 in this study to balance emphasis on large and small deviations.

$$\Delta_{ij} = \left|x_0^* - x_{ij}^*\right| \quad (3)$$

$$\xi_{ij} = \frac{\Delta_{min} + \Delta\zeta_{max}}{\Delta_{0i}(k) + \Delta\zeta_{max}} \quad (4)$$

Finally, the Grey Relational Grade (GRG) for each experimental trial was obtained by averaging the GRCs across all performance characteristics, as shown in (5). A higher GRG indicates superior overall performance. Here, y_i is the GRG of the i-th trial, n is the total number of response variables, and ξ_{ij} is the GRC value for the j-th performance characteristic. The parameter combination with the highest GRG was identified as the optimal setting, representing

the best trade-off across all mechanical responses measured.

$$y_i = \frac{1}{n}\sum_{j=1}^{n} \xi_{ij} \quad (5)$$

RESULTS AND DISCUSSION

Filament Dimension

Before evaluating the mechanical performance of the extruded recycled PLA–PETG filaments, dimensional accuracy was assessed to ensure compatibility with standard FDM 3D printers. Filament diameter was measured at nine equidistant points along each specimen, across three replications for each of the nine experimental runs.

The results are summarized in Table 3, which presents the average diameter and standard deviation for each run. While Run 8 exhibited the highest variation in diameter (SD = 0.184 mm), it remained within the acceptable tolerance band. In contrast, Runs 4 and 5 demonstrated the most consistent diameters, with standard deviations of 0.061 mm and 0.060 mm, respectively. Overall, all measured diameters fell within the acceptable range of 1.75 ± 0.2 mm, with mean values ranging from 1.633 mm to 1.704 mm.

Based on these results, all extruded filaments were deemed dimensionally suitable for 3D printing and proceeded to the next stage of analysis, which involved evaluating their mechanical performance—specifically, ultimate tensile strength and elongation.

Tensile Properties of Extruded Filament

The mechanical properties of the extruded rPLA–rPETG filaments were evaluated based on their ultimate tensile strength (UTS) and elongation at break.

Table 3. Average diameter measurements of the extruded filaments

Run	Mean Diameter (mm)	Standard Deviation (mm)
1	1.658	0.075
2	1.683	0.101
3	1.650	0.068
4	1.670	0.061
5	1.702	0.060
6	1.704	0.062
7	1.664	0.081
8	1.633	0.184
9	1.643	0.133

Table 4 presents the mean values of both responses across the nine experimental runs based on the L9 orthogonal array. Among all runs, Run 5 exhibited the highest UTS (0.1849 MPa), while Run 2 recorded the highest elongation (13.03%). Conversely, Run 3 consistently demonstrated the lowest performance in both metrics. This variation can be attributed to the combined influence of PLA content, extrusion temperature, and extrusion speed on the molecular structure and interlayer bonding of the filament. These are consistent with polymer blend behavior where processing parameters directly influence melt homogeneity, chain mobility, and the degree of interfacial bonding between immiscible phases [38][39].

A trade-off can be observed between tensile strength and elongation. For instance, Run 2, which had the highest elongation, achieved only moderate tensile strength. On the other hand, Run 5 attained the highest tensile strength but lower ductility. This suggests that parameter combinations that enhance strength may restrict polymer chain mobility, thus reducing elongation, and vice versa. Such opposing behavior reflects the inherent incompatibility of PLA and PETG, where stiffness increases with higher PLA contribution but at the cost of ductility due to reduced segmental motion and weaker phase adhesion.

To identify the individual parameter settings that produced the best performance for each response, the optimal runs were examined. As shown in Table 5, the best UTS was obtained from Run 5, corresponding to a PLA content of 30%, an extrusion temperature of 225 °C, and an extrusion speed of 475 mm/min. In contrast, the highest elongation was achieved in Run 2, which used 0% PLA content, the same extrusion temperature of 225 °C, and a lower speed of 387.5 mm/min.

Table 4. Average UTS and elongation of the extruded filament

Run	Mean UTS (MPa)	Mean Elongation (%)
1	0.109	9.11
2	0.147	13.03
3	0.026	1.10
4	0.049	2.33
5	0.185	8.83
6	0.147	9.85
7	0.057	3.29
8	0.106	4.63
9	0.113	8.03

These results show single-response optimization cannot capture the competing influence of processing conditions on strength versus ductility. The different conditions between the two responses highlight the trade off to optimized between the two and therefore a multi-response optimization is required to determine a balanced setting that satisfies both performance criteria.

Statistical Analysis and Optimization

Grey Relational Analysis (GRA)

GRA was applied to determine the optimal parameter combination that balances both UTS and elongation. The average values of UTS and elongation from each experimental run were normalized using the "larger-is-better" criterion (Table 6), allowing for cross-comparison between the two performance metrics. Following normalization, the GRC was calculated for each response, and the GRG was obtained by averaging the GRCs across both responses.

As shown in Table 7, Run 2 produced the highest GRG value (0.905), indicating the best overall performance when considering both strength and ductility. This was followed by Run 5 (GRG = 0.880) and Run 6 (GRG = 0.813). The lowest GRG was observed in Run 3, consistent with its poor mechanical performance in both metrics.

The main effects plot in Figure 4 show that the most influential parameter was extrusion temperature, followed by extrusion speed and PLA content. The optimal combination based on GRA is PLA content of 30%, extrusion temperature of 225 °C, and extrusion speed of 300 mm/min. The integration of Taguchi and GRA in this study is particularly relevant because the two mechanical responses (UTS and elongation) exhibit opposing trends; thus, GRA enables simultaneous evaluation without disproportionately favoring one property. This multi-response requirement differentiates the present study from earlier Taguchi–GRA optimizations that focused on single-response optimization or on blends with lower degradation levels and better miscibility.

Table 5. Best parameter settings for UTS and elongation

Variable	Best parameter	
	UTS	elongation
PLA Content	30	0
Extrusion Temperature (°C)	225	225
Extrusion Speed (mm/min)	475	387.5

Table 6. Calculation of Normalized S/N Ratio

Run	Ultimate Tensile Strength	Elongation
1	0.730	0.855
2	0.883	1.000
3	0.000	0.000
4	0.318	0.304
5	1.000	0.843
6	0.883	0.887
7	0.392	0.443
8	0.712	0.581
9	0.748	0.804

Tabel 7. Grey Relational Coefficient

Run	Ultimate Tensile Strength	Elongation	GRG	Rank
1	0.650	0.775	0.713	4
2	0.810	1.000	0.905	1
3	0.333	0.333	0.333	9
4	0.423	0.418	0.420	8
5	1.000	0.761	0.880	2
6	0.810	0.815	0.813	3
7	0.451	0.473	0.462	7
8	0.635	0.544	0.590	6
9	0.665	0.719	0.692	5

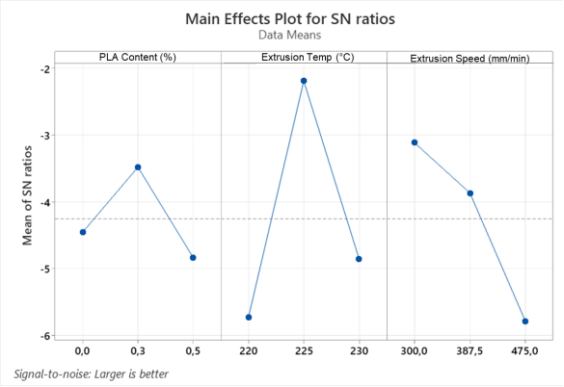

Figure 4. Main Effects Plot for the S/N Ratio of Grey Relational Analysis

These findings are consistent with the observed main effects trends, confirming that extrusion temperature has the most decisive influence on combined mechanical performance. The selected parameter settings that yielded the highest GRG are summarized in Table 8.

ANOVA

Before performing ANOVA, a normality test was conducted on the experimental data to ensure the assumptions of parametric analysis were satisfied. The results confirmed that both ultimate tensile strength (UTS) and elongation were approximately normally distributed, with p-values of 0.088 and >0.100, respectively.

ANOVA was then applied to assess the significance of each process parameter on the mechanical responses. As shown in Table 9, extrusion temperature had a statistically

significant effect on UTS (p = 0.000), followed by extrusion speed (p = 0.004), while PLA content showed no significant influence (p = 0.168). The significant contribution of extrusion temperature underscores its dominant role in enhancing melt flow uniformity and interlayer cohesion, illustrating that thermal energy is the primary factor governing tensile strength in mixed recycled filaments. Meanwhile, the non-significant effect of PLA content suggests that within the tested range, compositional variation does not substantially alter tensile strength due to the overriding impact of immiscibility.

In contrast, Table 10 shows that none of the parameters had a statistically significant effect on elongation at the 95% confidence level. However, extrusion temperature and speed exhibited relatively lower p-values (0.191 and 0.189, respectively). This indicates that elongation is more sensitive to complex interactions or microstructural defects not fully captured by the selected parameters, such as void formation, phase separation, or local brittleness induced by recycled feedstock degradation.

Validation Test

To validate the effectiveness of the optimized extrusion parameters obtained from GRA, tensile specimens were printed using the FDM technique. The best parameters were used to extrude filament, which was then printed into ASTM D638 Type IV specimens as described in the Method section. The printed parts were subjected to tensile testing to evaluate their mechanical performance.

Table 8. Best parameter settings based on Grey Relational Analysis

Variable	Selected value
PLA Content	30%
Extrusion Temperature (°C)	225℃
Extrusion Speed (mm/min)	300 mm/min

Table 9. Analysis of Variance for Ultimate Tensile Strength

Source	Df	Adj SS	Adj MS	F-Value	P-Value
PLA Content	2	0.08820	0.441	1.95	0.168
Extrusion Temp.	2	5.2545	2.6273	11.65	0.000
Extrusion Speed	2	3.2592	1.6296	7.22	0.004
Error	20	4.5120	0.2256		
Lack-of-Fit	2	2.5080	1.2540	11.26	0.001
Pure Error	18	2.0041	0.1113		
Total	26	13.9077			

Table 10. Analysis of Variance for Elongation

Source	Df	Adj SS	Adj MS	F-Value	P-Value
PLA Content	2	0.002799	0.001400	0.72	0.500
Extrusion Temp	2	0.007025	0.003513	1.80	0.191
Extrusion Speed	2	0.007074	0.007074	1.81	0.189
Error	20	0.039046	0.001952		
Lack-of-Fit	2	0.021482	0.010741	11.01	0.001
Pure Error	18	0.017564	0.000976		
Total	26	0.055944			

The results are presented in Figure 5, which compares the ultimate tensile strength (UTS) and elongation at break of the mixed rPETG–rPLA specimen with those of a commercial PETG specimen under the same testing conditions. As shown, the commercial PETG achieved a UTS of 44.81 MPa and an elongation of 7.47%, while the mixed rPETG–rPLA specimen reached only 7.50 MPa in UTS and 1.58% in elongation. The substantial performance gap reflects combined effects of chain scission due to prior thermal cycling, limited interfacial adhesion between PLA and PETG phases, and microvoid formation during extrusion and printing.

The predicted UTS and elongation for the rPETG–rPLA specimen, as shown in Table 11, were 0.17 MPa and 8.07%, respectively. The actual UTS far exceeded the prediction, but the elongation was considerably lower. This deviation indicates that GRA captured general trends but not microstructural variations, suggesting that fracture mechanisms in recycled blends are more sensitive to local defects and phase morphology than to average parameter effects.

Despite lower performance, the optimized recycled blend still demonstrated functional mechanical behavior suitable for low-load or non-structural applications such as prototyping components and non-load-bearing parts.

DISCUSSION

This study demonstrated the optimization of extrusion parameters for producing functional 3D printing filament from recycled PETG and PLA blends. Based on the Taguchi method and Grey Relational Analysis (GRA), the optimal combination—30% PLA content, 225 °C extrusion temperature, and 300 mm/min extrusion speed, yielded improved tensile properties across both performance indicators: ultimate tensile strength (UTS) and elongation.

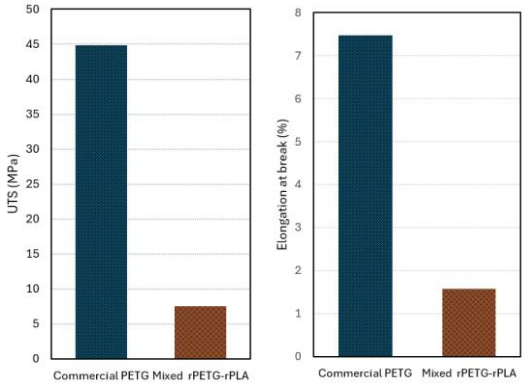

Figure 5. Comparison of tensile properties between commercial PETG and optimized rPETG–rPLA specimens: ultimate tensile strength (UTS, left) and elongation at break (right).

Table 11. Tensile Test Data for Specimens

Material Type	Commercial PETG	Mixed rPETG-rPLA
Ultimate Tensile Strength (Mpa)	44.81	7.50
Prediction UTS (Mpa)	NA	0.17
Elongation at Break (%)	7.47	1.58
Prediction Elongation (%)	NA	8.07

Compared with previous Taguchi–GRA studies, the contribution of this work lies in its application to a recycled PLA–PETG blend, a system known to exhibit immiscibility and variable material quality. While earlier research often examined single-material or less heterogeneous recycled feedstocks, this study applies Taguchi–GRA to a dual-feedstock blend that displays competing trends between strength and ductility. The findings show that the Taguchi–GRA framework remains effective for identifying balanced processing conditions even when the responses behave oppositely, thereby demonstrating its relevance in more complex recycled-material scenarios.

Similar optimization strategies have been shown to be effective in prior studies, such as the use of Taguchi-GRA to optimize recycled PETG and PLA blends, where results showed that rPETG performed best among the materials tested under optimized settings [49]. Validation tests using the optimized filament confirmed its printability and mechanical functionality, though with noticeable performance gaps compared to commercial PETG.

The results highlighted a trade-off between tensile strength and elongation. Specimens with higher UTS typically exhibited reduced elongation, suggesting that parameter combinations enhancing strength may limit polymer chain mobility, thereby reducing ductility. Among the three factors studied, extrusion temperature had the most significant influence on UTS, while extrusion speed appeared to be more influential for elongation. This aligns with previous studies reporting that extrusion temperature has the most significant effect on the mechanical performance of PETG composites, while printing speed and layer height more strongly impact ductility [50].

Compared to commercial PETG, the optimized rPETG–rPLA blend showed substantially lower mechanical performance. While commercial PETG achieved a UTS of 44.81 MPa and elongation of 7.47%, the printed recycled blend reached only 7.47 MPa in UTS and 1.58% in elongation. When benchmarked against previous studies (see Table 12), this performance is lower than reported values for 100% rPETG, which range from 12.9 MPa to 41.29 MPa in UTS and 5.51% in elongation. For example, Zisopol et al. reported a UTS of 41.29 MPa for 100% rPETG [51], while Nguyen et al. observed 12.9 ± 1.1 MPa [52]. Even rPLA alone can achieve UTS values of 16–24 MPa depending on printing infill and pattern settings [53]. The much lower UTS observed in this study suggests that degradation effects from both recycled components, along with poor interfacial compatibility in the rPETG–rPLA blend, significantly compromise mechanical performance. PETG and PLA are inherently immiscible, leading to poor interfacial adhesion in their blends. This immiscibility results in phase separation, which compromises the mechanical integrity of the composite [54]. These findings reinforce earlier studies reporting incompatibility in PLA–PETG blends [40][54]. while also extending prior knowledge by quantifying performance under extrusion conditions optimized via Taguchi–GRA.

It is also important to note that values reported for virgin PLA and PETG may derive from different runs for strength and elongation. For instance, the reported UTS of 54.39 MPa and elongation of 6.28% from Wang et al. (2020) were not measured from the same specimen [55]. This underscores the benefit of multi-response optimization approaches like GRA, which evaluate performance holistically.

The fracture surface analysis in Figure 6 offers further insight into the material behavior. The commercial PETG specimen exhibited smooth, uniform fracture morphology with well-fused layers, indicative of strong interlayer adhesion.

Table 12. Comparison of Research Results

Material	Ultimate Tensile Stength (MPa)	Elongation (%)	Ref.
PETG	35.46	NA	[69]
PLA	54.39	6.28	[62]
PLA-PETG (18% PETG)	48.43	15.70	[45]
rPLA-vPLA (50:50)	25.35 ± 1.98	2.90 ± 1.86	[19]
rPLA	16 -26	NA	[70]
rPETG (100%)	41.29	5.51	[58] [59]
rPETG (100%)	12.9 ± 1.1	NA	
This study	7.47	1.56	

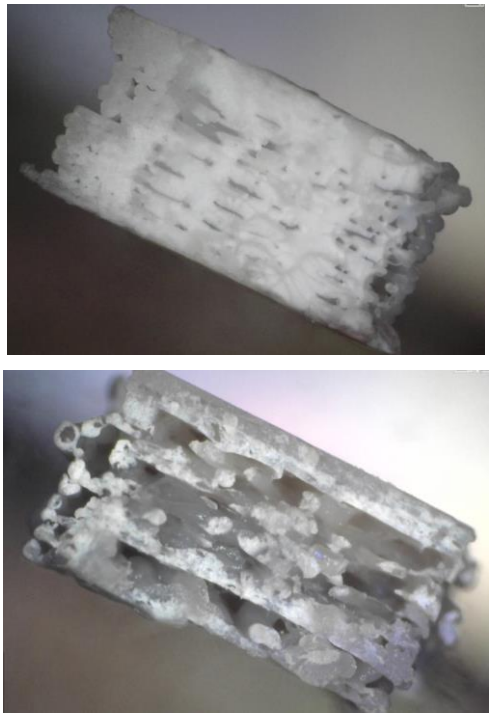

Figure 6. Fracture on printed specimens: commercial PETG (top) and rPETG-rPLA (bottom)

In contrast, the rPETG–rPLA sample displayed rougher, more irregular fracture surfaces with visible voids and delamination, signaling poor interlayer fusion and greater brittleness. These defects act as crack initiation points and hinder stress transfer across layers, explaining the significantly lower elongation and premature brittle failure in the recycled blend. This aligns with prior observations that blending PETG with PLA may reduce interlayer adhesion due to immiscibility, despite improved ductility [39]. The discrepancy between the predicted and actual values in the validation test—where predicted elongation was 8.07% but actual elongation was only 1.56%—may also stem from these morphological inconsistencies, as well as from moisture content, thermal degradation during reprocessing, or filament diameter fluctuation. Such variability highlights that microstructural imperfections can dominate failure behavior even when processing parameters are optimized.

Several experimental limitations should be acknowledged. Variations in filament diameter, moisture reabsorption after drying, and thermal degradation from repeated processing cycles may have influenced mechanical performance. Moreover, recycled feedstocks often contain inherent molecular-weight variability and contaminants that introduce heterogeneity not fully captured in the selected parameter set. These factors may contribute to deviations in predicted versus actual performance and should be considered in future work.

Despite its lower performance, the optimized rPETG–rPLA filament holds potential for low-stress or non-structural applications, particularly where sustainability and cost reduction are key priorities [18, 54, 56]. Examples include prototyping, conceptual models, packaging fixtures, or educational aids. The circular value of reusing waste material should not be understated, especially when aligned with environmental goals. Reusing materials helps reduce the volume of waste that ends up in landfills or incinerators, thereby decreasing harmful emissions such as carbon dioxide, nitrogen oxides, and methane [57][58]. It also creates new job opportunities in the recycling and waste management sectors, contributing to economic growth [59].

To improve material performance, future work may explore the use of compatibilizers or plasticizers to enhance interfacial bonding, as well as post-processing techniques such as annealing. A more granular examination of blend ratios, drying protocols, and extrusion stability is also recommended. Furthermore, thermal and rheological characterization could provide more profound understanding of blend interactions and processing windows.

CONCLUSION

This study successfully demonstrated the feasibility of producing 3D printing filament from recycled PETG and PLA blends using extrusion process optimization. By applying the Taguchi method combined with Grey Relational Analysis (GRA), the optimal extrusion parameters were identified as 30% PLA content, 225 °C extrusion temperature, and 300 mm/min extrusion speed. Under these optimized conditions, the filament achieved a UTS of 7.47 MPa and an elongation of 1.58%, representing a measurable

improvement over several non-optimized preliminary trials. This confirms the effectiveness of the combined Taguchi–GRA framework for multi-response optimization of recycled polymer blends.

Despite showing lower mechanical properties compared to commercial PETG and previously reported recycled materials, the optimized rPETG–rPLA filament demonstrated sufficient dimensional accuracy and printability, making it suitable for low-stress and non-structural applications. Fractographic analysis revealed that weak interlayer bonding and morphological inconsistencies contribute to mechanical limitations, highlighting the challenges of recycling immiscible polymer blends. The methodological contribution of this work lies in applying Taguchi–GRA to a dual-feedstock recycled system with intrinsic immiscibility, demonstrating its ability to identify balanced conditions even when tensile strength and ductility exhibit competing trends.

This research underscores the importance of combining statistical optimization with multi-response analysis to improve the quality of recycled materials in additive manufacturing. Future work should incorporate deeper thermal, rheological, and microstructural characterization, as well as the potential use of compatibilizers, chain extenders, or post-processing treatments to improve interlayer adhesion. Broader environmental implications also merit emphasis: optimizing recycled PETG–PLA blends contribute to waste reduction and supports circular material flows, offering a more sustainable pathway for filament production in additive manufacturing.

REFERENCES

[1] J. C. Vasco, “Additive manufacturing for the automotive industry,” in *Additive Manufacturing*, Elsevier, 2021, pp. 505–530, doi: 10.1016/B978-0-12-818411-0.00010-0.

[2] N. Zhao, M. Parthasarathy, S. Patil, D. Coates, K. Myers, H. Zhu, and W. Li, “Direct additive manufacturing of metal parts for automotive applications,” *Journal of Manufacturing Systems*, vol. 68, pp. 368–375, 2023, doi: 10.1016/j.jmsy.2023.04.008.

[3] M. Khorasani, A. Ghasemi, B. Rolfe, and I. Gibson, “Additive manufacturing: A powerful tool for the aerospace industry,” *Rapid Prototyping Journal*, vol. 28, no. 1, pp. 87–100, 2022, doi: 10.1108/RPJ-01-2021-0009.

[4] C. Radhika, R. Shanmugam, M. Ramoni, and B. K. Gnanavel, “A review on additive manufacturing for aerospace application,” *Materials Research Express*, vol. 11, no. 2, p. 022001, 2024, doi: 10.1088/2053-1591/ad21ad.

[5] E. R. Ghomi, F. Khosravi, R. E. Neisiany, S. Singh, and S. Ramakrishna, “Future of additive manufacturing in healthcare,” *Current Opinion in Biomedical Engineering*, vol. 17, p. 100255, 2021, doi: 10.1016/j.cobme.2020.100255.

[6] A. B. Singh, “Transforming healthcare: A review of additive manufacturing applications in the healthcare sector,” *Engineering Proceedings*, vol. 72, no. 1, p. 2, 2024, doi: 10.3390/engproc2024072002.

[7] N. Sethuraman, A. K. Parlaktürk, and J. M. Swaminathan, “Personal fabrication as an operational strategy: Value of delegating production to customer using 3D printing,” *Production and Operations Management*, vol. 32, no. 7, pp. 2362–2375, 2023, doi: 10.1111/poms.13981.

[8] M. Jayakrishna, M. Vijay, and B. Khan, “An overview of extensive analysis of 3D printing applications in the manufacturing sector,” *Journal of Engineering*, vol. 2023, no. 1, p. 7465737, 2023, doi: 10.1155/2023/7465737.

[9] K. Saptaji et al., “Improvement of ankle foot orthotics fabrication using 3D printing method,” *SINERGI*, vol. 28, no. 3, 2024, doi: 10.22441/sinergi.2024.3.015.

[10] T. J. Suteja, R. Handoko, and A. Soesanti, “Experimental study and optimisation of flexural properties of 3D-printed polylactic acid for energy-storing-and-returning prosthetic foot,” *SINERGI*, vol. 29, no. 3, 2025, doi: 10.22441/sinergi.2025.3.015.

[11] L. Sun, “3D printing and additive manufacturing in fashion,” in *Leading Edge Technologies in Fashion Innovation: Product Design and Development Process from Materials to the End Products to Consumers*, Y. A. Lee, Ed. Cham, Switzerland: Palgrave Macmillan, 2022, pp. 59–74, doi: 10.1007/978-3-030-91135-5_4.

[12] Fact.MR, “Additive manufacturing market,” Fact.MR, 2025. [Online]. Available: https://www.factmr.com/report/additive-manufacturing-market. [Accessed: May 12, 2025].

[13] K. Sathish, R. Panneerselvam, S. S. Kumar, and M. K. Selvam, “A comparative study on subtractive manufacturing and additive manufacturing,” *Advances in Materials Science and Engineering*, vol. 2022, no. 1, p. 6892641, 2022, doi: 10.1155/2022/6892641.

[14] S. Srivastava, A. Sharma, and V. Kushvaha, “Applications of additive manufacturing,” in *Additive and Subtractive Manufacturing of Composites*, S. M. Rangappa, M. K. Gupta,

S. Siengchin, and Q. Song, Eds. Singapore: Springer, 2021, pp. 201–226, doi: 10.1007/978-981-16-3184-9_8.
[15] J. I. Sword, A. Galloway, and A. Toumpis, "An environmental impact comparison between wire+ arc additive manufacture and forging for the production of a titanium component," *Sustainable Materials and Technologies*, vol. 36, p. e00600, 2023, doi: 10.1016/j.susmat.2023.e00600.
[16] G. Atakok, M. Kam, and H. B. Koc, "A review of mechanical and thermal properties of products printed with recycled filaments for use in 3D printers," *Surface Review and Letters*, vol. 29, no. 02, p. 2230002, 2022, doi: 10.1142/S0218625X22300027.
[17] J. Zimmerman, "Campus sustainability in action: Recycling 3D printing waste," NC State University, 2025. [Online]. Available: https://cnr.ncsu.edu/fb/news/2025/03/campus-sustainability-in-action-recycling-3d-printing-waste/. [Accessed: May 12, 2025].
[18] M. R. Hasan, I. J. Davies, A. Pramanik, M. John, and W. K. Biswas, "Recycling Post-Consumed Polylactic Acid Waste Through Three-Dimensional Printing: Technical vs. Resource Efficiency Benefits," *Sustainability*, vol. 17, no. 6, p. 2484, 2025, doi: 10.3390/su17062484.
[19] A. Yadav, P. Rohru, A. Babbar, R. Kumar, N. Ranjan, J. S. Chohan, R. Kumar, and M. Gupta, "Fused filament fabrication: A state-of-the-art review of the technology, materials, properties and defects," *International Journal on Interactive Design and Manufacturing*, vol. 17, no. 6, pp. 2867–2889, 2023, doi: 10.1007/s12008-022-01026-5.
[20] S. W. T. Tientcheu, J. M. Djouda, M. A. Bouaziz, and E. Lacazedieu, "A review on fused deposition modeling materials with analysis of key process parameters influence on mechanical properties," *The International Journal of Advanced Manufacturing Technology*, vol. 130, no. 5, pp. 2119–2158, 2024, doi: 10.1007/s00170-023-12823-x.
[21] M. Kopar and A. R. Yildiz, "Experimental investigation of mechanical properties of PLA, ABS, and PETG 3-d printing materials using fused deposition modeling technique," *Materials Testing*, vol. 65, no. 12, pp. 1795–1804, 2023, doi: 10.1515/mt-2023-0202.
[22] G. Bürge, E. Aytaç, A. Evcil, and M. A. Savaş, "An investigation on mechanical properties of PLA produced by 3D printing as an implant material," in *2020 4th International Symposium on Multidisciplinary Studies and Innovative Technologies (ISMSIT)*, IEEE, 2020, pp. 1–6, doi: 10.1109/ismsit50672.2020.9254387.
[23] S. Elhady, I. A. B. D. Ellatif, K. M. Abdelrahman, A. S. Mostaf, and I. S. Fahim, "Innovations in 3D Printing-Assisted Biopolymers for Biomedical Applications," *Sustainable 3D Printing for Innovative Biopolymer Production and Applications*, pp. 95–116, 2025, doi: 10.1002/9781119792314.ch5.
[24] X. Chen, G. Chen, G. Wang, P. Zhu, and C. Gao, "Recent progress on 3D-printed polylactic acid and its applications in bone repair," *Advanced Engineering Materials*, vol. 22, no. 4, p. 1901065, 2020, doi: 10.1002/adem.201901065.
[25] H. Schneevogt, K. Stelzner, B. Yilmaz, B. E. Abali, A. Klunker, and C. Völlmecke, "Sustainability in additive manufacturing: Exploring the mechanical potential of recycled PET filaments," *Composites and Advanced Materials*, vol. 30, p. 26349833211000063, 2021, doi: 10.1177/26349833211000063.
[26] G. J. P. Bex, B. L. J. Ingenhut, T. Ten Cate, M. Sezen, and G. Ozkoc, "Sustainable approach to produce 3D-printed continuous carbon fiber composites: A comparison of virgin and recycled PETG," *Polymer Composites*, vol. 42, no. 9, pp. 4253–4264, 2021, doi: 10.1002/pc.26143.
[27] G. Holcomb, E. B. Caldona, X. Cheng, and R. C. Advincula, "On the optimized 3D printing and post-processing of PETG materials," *MRS Communications*, vol. 12, no. 3, pp. 381–387, 2022, doi: 10.1557/s43579-022-00188-3.
[28] H.-H. Tsai, S.-J. Wu, Y.-D. Wu, and W.-Z. Hong, "Feasibility study on the fused filaments of injection-molding-grade poly(ethylene terephthalate) for 3D printing," *Polymers*, vol. 14, no. 11, p. 2276, 2022, doi: 10.3390/polym14112276.
[29] S. Momeni, K. Craplewe, M. Safder, S. Luz, D. Sauvageau, and A. Elias, "Accelerating the biodegradation of poly(lactic acid) through the inclusion of plant fibers: A review of recent advances," *ACS Sustainable Chemistry & Engineering*, vol. 11, no. 42, pp. 15146–15170, 2023, doi: 10.1021/acssuschemeng.3c04240.
[30] P. C. Mayekar and R. Auras, "Accelerating biodegradation: Enhancing poly(lactic acid) breakdown at mesophilic environmental conditions with biostimulants," *Macromolecular Rapid Communications*, vol. 45, no. 7, p. 2300641, 2024, doi: 10.1002/marc.202300641.

[31] P. C. Mayekar and R. Auras, “Speeding it up: Dual effects of biostimulants and iron on the biodegradation of poly(lactic acid) at mesophilic conditions,” *Environmental Science: Processes & Impacts*, vol. 26, no. 3, pp. 530–539, 2024, doi: 10.1039/D3EM00534H.

[32] I. Rahman and A. E. Gandasasmita, “Environmental impact analysis of polyethylene terephthalate plastic recycling process using life-cycle assessment,” in *AIP Conference Proceedings*, vol. 2710, no. 1, p. 050015, 2024, doi: 10.1063/5.0144971.

[33] L. Porojan, F. R. Toma, M. I. Gherban, R. D. Vasiliu, and A. Matichescu, “Surface Topography of Thermoplastic Appliance Materials Related to Sorption and Solubility in Artificial Saliva,” *Biomimetics*, vol. 9, no. 7, p. 379, 2024, doi: 10.3390/biomimetics9070379.

[34] W. Li, X. Zhao, Y. Liu, Y. Ouyang, W. Li, D. Chen, and D. Ye, “Hygrothermal aging behavior and flexural property of carbon fiber-reinforced polyethylene terephthalate glycol composites,” *Textile Research Journal*, vol. 93, no. 5–6, pp. 1005–1018, 2023, doi: 10.1177/00405175221126005.

[35] Ç. Bolat, B. Ergene, and H. Ispartalı, “A comparative analysis of the effect of post-production treatments and layer thickness on tensile and impact properties of additively manufactured polymers,” *International Polymer Processing*, vol. 38, no. 2, pp. 244–256, 2023, doi: 10.1515/ipp-2022-4267.

[36] L. Marsavina, V. Dohan, and S.V. Galatanu, “Mechanical evaluation of recycled PETG filament for 3D printing,” *Fracture and Structural Integrity*, vol. 18, no. 70, pp. 310–321, 2024, doi: 10.3221/IGF-ESIS.70.18.

[37] N. H. Mohd Rosmmi, Z. I. Khan, Z. Mohamad, R. Abd Majid, N. Othman, S. H. Che Man, and K. J. Abd Karim, “Impact strength and morphology of sustainably sourced recycling polyethylene terephthalate blends,” *Chemical Engineering Transactions*, vol. 83, pp. 265–270, 2021, doi: 10.3303/CET2183045.

[38] F. Richter and D. Wu, “Interfacial adhesion between dissimilar thermoplastics fabricated via material extrusion-based multi-material additive manufacturing,” *Materials & Design*, vol. 252, p. 113688, 2025, doi: 10.1016/j.matdes.2025.113688.

[39] K. Bouguermouh, M. Habibi, L. Laperrière, Z. Li, and Y. Abdin, “4D-printed PLA-PETG polymer blends: comprehensive analysis of thermal, mechanical, and shape memory performances,” *J. Mater. Sci.*, vol. 59, no. 25, pp. 11596–11613, 2024, doi: 10.1007/s10853-024-09862-4.

[40] A. Thirugnanasambandam, H. Dutta, C. L. Gnanasagaran, and J. D. Kechagias, “Development of 3D printed novel multi-polymer component based on blended filaments of polylactic acid and polyethylene terephthalate glycol,” *Progress in Additive Manufacturing*, vol. 10, no. 2, pp. 1147–1160, 2025, doi: 10.1007/s40964-024-00695-w.

[41] X. Ang, C. K. Owi, J. Y. Tey, W. H. Yeo, P. Yee, and K. Shak, “3D printing of composite material through blending of PLA and PETG using fused deposition modelling,” in *AIP Conference Proceedings*, AIP Publishing, 2023, doi: 10.1063/5.0165316.

[42] D. Ying, P. Pasam, S. Addimulam, and V. M. Natakam, “The role of polymer blends in enhancing the properties of recycled rubber,” *ABC Journal of Advanced Research*, vol. 11, no. 2, pp. 115–126, 2022, doi: 10.18034/abcjar.v11i2.757.

[43] M. I. Ramli, A. M. Choudhury, D. L. J. Choong, T. J. Jun, N. R. R. Royan, and M. A. F. M. Tajudin, “PLA/Wollastonite Composite Filaments for 3D Printing Application: Rheological Properties and Extrusion,” *Jurnal Kejuruteraan*, vol. 36, no. 5, pp. 2097–2106, 2024, doi: 10.17576/jkukm-2024-36(5)-26.

[44] C. Wang *et al.*, “Preparation and properties of PP/PET filament blends for 3D printing applications,” *Cailiao Gongcheng/Journal of Materials Engineering*, vol. 52, no. 4, pp. 218–224, 2024, doi: 10.11868/j.issn.1001-4381.2022.000122.

[45] L. Firtikiadis, A. Tzotzis, P. Kyratsis, and N. Efkolidis, “Response Surface Methodology (RSM)-Based Evaluation of the 3D-Printed Recycled-PETG Tensile Strength,” *Applied Mechanics*, vol. 5, no. 4, pp. 924–937, 2024, doi: 10.3390/applmech5040051.

[46] M. R. Hasan, I. J. Davies, A. Pramanik, M. John, and W. K. Biswas, “Potential of recycled PLA in 3D printing: A review,” *Sustainable manufacturing and service economics*, vol. 3, p. 100020, 2024, doi: 10.1016/j.smse.2024.100020.

[47] H. Tebassi, M. A. Yallese, and S. Belhadi, “Optimization and machinability assessment at the optimal solutions across Taguchi OA, GRA, and BBD: An overall view,” *Arabian Journal for Science and Engineering*, vol. 48, no. 9, pp. 12455–12483, 2023, doi: 10.1007/s13369-023-07825-6.

[48] B. E. Yuce, “Optimization of critical system outputs of the Stirling cycle using Taguchi-based grey relational analysis,” *Proceedings of the Institution of Mechanical Engineers,*

Part E: Journal of Process Mechanical Engineering, pp. 1–16, 2024, doi: 10.1177/09544089241281983.
[49] A. C. Igwe and K. D. Oniko, "Investigation for an alternative material for the development of a clubfoot brace to improve sustainability," *Journal of Materials Engineering and Performance*, vol. 33, no. 2, pp. 906–924, 2024, doi: 10.1007/s11665-023-08012-2.
[50] S. Valvez, A. P. Silva, and P. N. B. Reis, "Optimization of printing parameters to maximize the mechanical properties of 3D-printed PETG-based parts," *Polymers*, vol. 14, no. 13, p. 2564, 2022, doi: 10.3390/polym14132564.
[51] D. G. Zisopol, M. Minescu, and D. V. Iacob, "A Study on the Tensile Behavior of Specimens Manufactured by FDM from Recycled PETG in the Context of the Circular Economy Transition," *Engineering, Technology & Applied Science Research*, vol. 14, no. 6, pp. 18681–18687, 2024, doi: 10.48084/etasr.8927.
[52] P. Q. K. Nguyen, T. D. Tran, H. T. Nguyen, M. T. Pham, and D. H. Nguyen, "Influences of printing parameters on mechanical properties of recycled PET and PETG using fused granular fabrication technique," *Polymer Testing*, vol. 132, p. 108390, 2024, doi: 10.1016/j.polymertesting.2024.108390.
[53] S. L. Rodríguez-Reyna, J. H. Díaz-Aguilera, J. P. García-Contreras, and F. Tapia, "Evaluation of the mechanical behavior of fused deposition modeling (FDM)-printed virgin and recycled PLA parts using factorial design," *MRS Advances*, vol. 9, no. 3, pp. 187–192, 2024, doi: 10.1557/s43580-023-00743-7.
[54] K. Bouguermouh, M. Habibi, L. Laperrière, Z. Li, and Y. Abdin, "Designing advanced 4D printing thermo-sensitive shape memory polymer blends for enhanced mechanical and shape memory performances," *Progress in Additive Manufacturing*, vol. 10, no. 9, pp. 6507–6526, 2025, doi: 10.1007/s40964-025-00989-7.
[55] S. Wang, Y. Ma, Z. Deng, S. Zhang, and J. Cai, "Effects of fused deposition modeling process parameters on tensile and dynamic mechanical properties of 3D-printed polylactic acid materials," *Polymer Testing*, vol. 86, p. 106483, 2020, doi: 10.1016/j.polymertesting.2020.106483.
[56] A. A. Bakır, R. Atik, and S. Özerinç, "Effect of fused deposition modeling process parameters on the mechanical properties of recycled polyethylene terephthalate parts," *Journal of Applied Polymer Science*, vol. 138, no. 3, p. 49709, 2021, doi: 10.1002/app.49709.
[57] L. S. Ani, L. Budovich, N. S. Klunko, G. U. Jumanazarova, K. Nasurova, and K. Asatullaev, "Reduction of cost and emissions by using recycling and waste management system," *Brazilian Journal of Biology*, vol. 83, p. e279565, 2023, doi: 10.1590/1519-6984.279565.
[58] A. Srivastava, S. Pandey, R. Shahwal, and A. Sur, "Recycling of waste into useful materials and their energy applications," in *Microbial Niche Nexus Sustaining Environmental Biological Wastewater and Water-Energy-Environment Nexus*, Springer, 2025, pp. 251–296, doi: 10.1007/978-3-031-62660-9_11.
[59] H. K. Kavuş, Y. Erköse, and D. Eryar, "Driving green job opportunities in sustainable waste management through co-production strategies: Informal recycling workers, municipalities, and the national agenda—A case study of İzmir," *Social Sciences*, vol. 12, no. 7, p. 387, 2023, doi: 10.3390/socsci12070387.
[60] B. Mallikarjuna, V. Mallesh, M. S. Vardhan, H. G. Vadivudaiyanayak, and P. G. S. Datta, "Effect of Process Parameters on Mechanical Properties in Fused Deposition Modelling of Polyethylene Terephthalate Glycol," *Procedia Structural Integrity*, vol. 56, pp. 160–166, 2024, doi: 10.1016/j.prostr.2024.02.051.
[61] L. Rodríguez-Parada, S. de la Rosa, and P. F. Mayuet, "Influence of 3D-printed TPU properties for the design of elastic products," *Polymers*, vol. 13, no. 15, p. 2519, 2021, doi: 10.3390/polym13152519.